

## Meandering instability of a spiral interface in the free boundary limit

Igor Mitkov,<sup>1</sup> Igor Aranson,<sup>2</sup> and David Kessler<sup>2</sup>

<sup>1</sup>*Racah Institute of Physics, The Hebrew University of Jerusalem, 91904 Jerusalem, Israel*

<sup>2</sup>*Department of Physics, Bar-Ilan University, Ramat Gan 52900, Israel*

(Received 27 August 1996)

The two-component reaction-diffusion excitable medium is treated numerically in the free boundary limit for the fast field. We find that the spiral interface is stable for a sufficiently high diffusion constant of the slow field. The spiral wave (interface) undergoes a core-meander instability via a forward Hopf bifurcation as the diffusion constant decreases. A further decrease of the diffusion constant is found to result in the onset of hypermeandering and spiral breakup. We demonstrate quantitative convergence of the dynamics of reaction-diffusion system to its free boundary limit. [S1063-651X(96)02912-1]

PACS number(s): 05.40.+j, 82.40.Fp

### I. INTRODUCTION

Spiral waves arising in two-dimensional (2D) excitable media currently attract a great deal of attention. These spirals appear in the well-known Belousov-Zhabotinsky reaction [1], in the catalysis of CO on Pt substrates [2], in the electrical activity of heart tissues [3], in the aggregation of amoebae colonies [4], etc. Excitable reaction-diffusion systems have been intensively studied both experimentally and analytically. Significant progress has been achieved through detailed numerical and analytical investigations of generic reaction-diffusion models [5–7] and canonical experimental systems [1,2]. It was established that the spirals can exhibit rich dynamic behavior ranging from periodic and quasiperiodic meandering to chaotic hypermeandering and spiral breakup under certain conditions.

The simplest (yet nontrivial) theory of wave propagation in excitable media consists of a pair of coupled reaction-diffusion equations for a fast field  $u$  (activator) and a slow field  $v$  (inhibitor), respectively [7,8],

$$\partial_t u = \epsilon \nabla^2 u + \frac{f(u, v)}{\epsilon}, \quad (1)$$

$$\partial_t v = \delta \epsilon \nabla^2 v + g(u, v), \quad (2)$$

where  $\epsilon$  is a positive parameter and  $\delta = D_v/D_u$  is the ratio of diffusion coefficients of the variables  $v$  and  $u$ . In the well-known FitzHugh-Nagumo (FN) model [9]  $f = 3u - u^3 - v$  and  $g = u - \gamma v + \Delta$ , with the parameters  $\gamma$  and  $\Delta$  governing the kinetics of the medium.

The behavior of the reaction-diffusion system modeled by Eqs. (1) and (2) is the subject of intensive investigation. The meandering instability of the spiral core was established both by direct numerical simulations [10,11] and by numerical solution of the linearized problem [12]. However, the above methods are restricted for not too small value of  $\epsilon$ . A comprehensive understanding of the spiral dynamics in the true asymptotic limit of small  $\epsilon$  is still lacking.

In most practically important cases the parameter  $\epsilon \ll 1$  (typically  $\epsilon \sim 10^{-4} - 10^{-2}$ ). This allows an effective reduction of the dynamics of a two-component medium to a *free boundary problem* for a narrow  $O(\epsilon)$  interface separating

regions of “excited” and “quiescent” phases of the fast field  $u$  coupled with the slowly varying field  $v$ . The dynamics of the curved interface is then given by the eikonal equation

$$c_n = c(v_I) - \epsilon k, \quad (3)$$

where  $v_I$  is the value of field  $v$  at the interface,  $c(v_I)$  is the interfacial velocity in the 1D case (found from a solvability condition of the corresponding one-dimensional problem),  $c_n$  is the velocity normal to the interface, and  $k$  is the local curvature of the interface [7,8]. Moreover, for  $\epsilon \ll 1$ ,  $v$  deviates only slightly from the “stall” value  $v_s$ , defined by  $c(v_s) = 0$ . In the limit of very small  $\epsilon$  the equations can be drastically simplified, bringing the system to a generic form. This can be done using a scaling, suggested by Fife [13]:  $v - v_s = \epsilon^{1/3} \tilde{v}$ ,  $x = \epsilon^{2/3} \tilde{x}$ ,  $t = \epsilon^{1/3} \tilde{t}$ , and  $c(v_I) \approx \epsilon^{1/3} c_v \tilde{v}_I$ , where  $c_v \equiv dc(v)/dv|_{v=v_s}$ ,  $[v_s]$  and  $c_v$  are constants defined by particular functions  $f(u, v)$  and  $g(u, v)$  in Eqs. (1) and (2); for instance, in the FN model  $v_s = 0$  and  $c_v = -1/\sqrt{2}$ . After dropping the tildes, the transformed system reads [to  $O(\epsilon^{1/3})$ ]

$$\partial_t v = g^\pm + \delta \Delta v - \alpha^\pm \epsilon^{1/3} v, \quad (4)$$

$$c_n = c_v v_I - k, \quad (5)$$

where the signs  $+$  and  $-$  correspond to the excited and quiescent regions, respectively.  $g^\pm \equiv g(u^\pm(v_s), v_s) = \text{const}$  and  $\alpha^\pm = -dg^\pm/dv_s = \text{const}$ . For convenience  $g^\pm$  may be normalized by choosing  $g^+ - g^- = 1$ , which, in the zeroth order of  $\epsilon^{1/3}$ , leaves only two independent dynamical parameters in Eqs. (4) and (5), which are  $g^+$  and  $\delta$ . In a true Fife limit of  $\epsilon^{1/3} \ll 1$ , the last term in Eq. (4) can be dropped and the system becomes universal (or model independent) [13]. However, even for very small  $\epsilon \sim 10^{-4} - 10^{-3}$ , the last term is approximately  $\epsilon^{1/3}$ , which is of order 0.1 and therefore is not formally *small numerically*. As a result, significant numerical discrepancies between the behavior of the reaction-diffusion system (1) and (2) and the simplified model (4) and (5) may have originated from neglecting this term.

The diffusionless ( $\delta = 0$ ) free boundary problem is not self-consistent since the interface develops a cusp (region of

infinite curvature) at the spiral tip. This singularity can be avoided by either including finite diffusion in the slow variable ( $\delta \neq 0$ ) or taking into account the finite value of  $\epsilon$  at the cusp. The latter approach is much more complicated since it breaks locally the interfacial approximation, and we will concentrate entirely on the former case.

In the limit of  $\delta \ll 1$  but  $\delta \gg \epsilon$ , the problems of spiral selection and stability can be solved fully analytically [5,14]. However, analytic results for this limit always predict a single unstable mode of the spiral, which is contradictory to the fact that in numerical simulations and in experiments the spiral undergoes a Hopf bifurcation from steady rotation of the core to meandering, which represents a pair of conjugate unstable modes.

The (quasistationary) finite  $\delta$  free boundary problem was recently considered by Kessler and Kupferman [15,16]. They have solved problem of the frequency selection and the stability of the spiral using a different numerical approach [15]. They have also found the Hopf bifurcation at finite  $\delta$ .

However, important questions such as the long-time spiral behavior and the emergence of spiral from ‘‘nonspiral’’ initial conditions cannot be answered in the framework of quasistationary theory. In particular, it is not clear whether the instability found in [16] really leads to supercritical bifurcation or destroys the spiral as happens in the complex Ginzburg-Landau equation [17]. For this purpose one needs to solve the time-dependent free boundary problem (4) and (5).

In the present paper we treat the free-boundary problem by direct simulations of Eqs. (4) and (5) for finite  $\delta$ . We consider a nonclosed interface in a rectangular domain. We develop a numerical procedure to handle the reconnection and tearing off of the interface at the domain boundary, which is a new element in the numerical study of free boundary problems (previous methods were restricted to closed interfaces [18,19]). We present numerical evidence that the finite diffusion free boundary problem is sufficient to describe the formation of spiral waves in the generic reaction-diffusion excitable media. We have found that in a certain region of parameters  $g^+, \delta$  generic initial conditions evolve into a steadily rotating spiral. We also found that the spiral wave undergoes a core-meander instability via a forward Hopf bifurcation as  $\delta$  decreases. Therefore, near the threshold the instability is saturated and does not destroy the spiral. A further decrease of  $\delta$  results in a transition to hypermeandering and finally to the breakup of the spiral. Our results are consistent with numerical simulations of the original reaction-diffusion system and experiments and therefore resolve the existing controversy in the theory of spiral waves in the free boundary limit.

## II. NUMERICAL METHODS

We perform simulations of the system (4) and (5) for  $\epsilon=0$ , using a mixed technique, which solves the diffusion equation (4) for the field  $v$ , determined at the sites of a square grid, and the nonlinear interfacial equation (5), separating excited and quiescent regions. The source term in Eq. (4) takes the values  $g^+(g^-)$  in the excited (quiescent) region, respectively. The curved interface is determined by points distributed along the interface, which is general do not

coincide with the grid sites. These interfacial points are moved according to Eq. (5). The details of the numerical technique are described in the Appendix.

We consider a square domain on a 2D grid, with the interface attached with both of its ends to the boundaries of the domain. We choose *no-flux* boundary conditions for  $v$  (i.e.,  $\nabla v$  on the domain boundary is always parallel to the boundary), which forces the interface to be perpendicular to the boundary at both points of attachment. Interfacial points are distributed along the interface, with their positions parametrized by the arclength  $s$ . After the spiral is formed, we call the part of the interface where the excited region is convex into the quiescent one the *front* and the part where it is concave the *back*. We choose the arclength to increase from the front end of the interface to its back end.

We have found that there is a numerical instability of the points along the interface, which leads to the ‘‘leakage’’ of the points out of the tip. This can be explained by the fact that the error in the calculation of curvatures and interfacial normals increases with curvature. In order to suppress this instability, we redistribute the points along the interface at every time step at equal distances along the interface.

The situation when an interior point of the interface touches the domain boundary needs special consideration. When such an event occurs, we cut the part of the interface beyond the new point of attachment to the boundary. Formally we would have to keep track of the remainder thereafter, but, as we know from the theory of generic reaction-diffusion excitable media (1) and (2), the influence of the remainder decays superexponentially [20]. Moreover, due to the active (or invasive) character of the spiral, which emits waves outward, the influence of the cut pieces is vanishingly small. Indeed, the perturbations produced by the cut piece propagate against the direction of the group velocity and rapidly decay. After such a cutoff is performed we have to rebuild the function  $g^\pm(x,y)$  in the whole bulk. The position of the spiral’s core is tracked as a point with zero normal velocity  $c_n$  by linear (cubic) interpolation between corresponding interfacial points, nearest to the core.

## III. MEANDERING INSTABILITY OF THE SPIRAL’S CORE

We have performed numerical simulations, using the described algorithm. We have studied systematically the dynamics of spiral in a wide range of parameters  $g^+, \delta$ . In order to generate stationary spiral solution we took generic nonspiral initial conditions for the interface (for example, a straight line). For sufficiently large values of  $\delta$  (see below) these initial conditions gradually evolved to a steadily rotating spiral. A stable spiral solution, obtained in this way, is shown in Fig. 1.

However, we have observed a core instability leading to meandering as  $\delta$  decreases. A typical trajectory of the unstable (meandering) spiral core is given in Fig. 2(a). We have verified by systematic control of the amplitude of the core meander that the instability occurs via a forward Hopf-like bifurcation, as it is observed in direct numerical simulations of the Eqs. (1) and (2) and experiments. The stability limit of the core meander in the  $\delta$ - $g^+$  plane is shown in Fig. 3. Near the threshold this instability is saturated at some finite radius

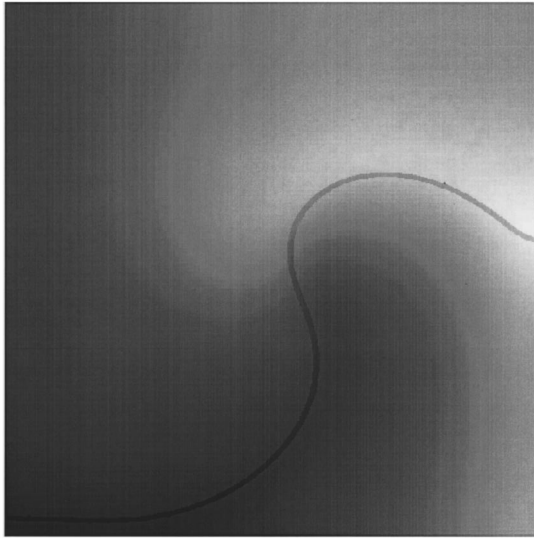


FIG. 1. Gray-coded snapshot of  $v$  field (black corresponds to the maximum value and white to the minimum value) and the interface in free boundary simulations. The parameters of the simulations are the square domain,  $20 \times 20$ ; number of grid points,  $129 \times 129$ ;  $\delta=0.3$ ;  $g^+=0.63$ ;  $c_v=-1/\sqrt{2}$ ; and the interface presented contains 155 interfacial points.

of the core meandering and does not destroy the spiral. A further decrease of  $\delta$  leads to a transition to hypermeandering [Fig. 2(b)], when many core modes are excited simultaneously. In this case the spiral's core performs a very complicated (nonperiodic) motion. Finally, for a very small diffusion the radius of the meandering becomes very large and the spiral annihilates at the boundary. It is plausible to assume that the radius of meander diverges at some finite value of  $\delta$ , which could be a fingerprint of the stationary instability of the spiral core found in the small- $\delta$  limit [5].

#### IV. COMPARISON WITH THE DYNAMICS OF THE REACTION-DIFFUSION SYSTEM

We have verified our results by the direct simulations of the original model (1) and (2) for finite  $\epsilon$ . We applied the EZ-spiral code of Barkley [11] for the model given by the functions  $f(u,v)=u(u-1)[u-u_{th}(v)]$  and  $g(u,v)=u-v$ , where  $u_{th}(v)=(v+b)/a$ . In this model  $g^+=1-a/2+b$ ,  $g^-=g^+-1$ , and  $c_v=-\sqrt{2}/a$ . We can see very slow convergence of the bifurcation lines obtained from the Eqs. (1) and (2) to that of the free boundary problem as  $\epsilon$  decreases (see Fig. 3). It is technically difficult to obtain quantitative agreement for  $\epsilon=0$  because it would require very small  $\epsilon$  ( $\sim 10^{-6}$ ), which makes Barkley's code drastically time consuming.

In order to reduce the discrepancy between the reaction-diffusion system and the free boundary problem due to finite  $\epsilon^{1/3}$ , we took into account the leading correction  $-\alpha^\pm \epsilon^{1/3} v$  [the last term in Eq. (4)]. The constants  $\alpha^\pm$  are determined by the particular model. In Barkley's model  $\alpha^\pm \equiv \alpha = 1$  and the value of  $c_v$  equals  $-\sqrt{2}/a$ , which is different from that for the FN model, given by  $c_v = -1/\sqrt{2}$ . In the zeroth-order problem (4) and (5)  $c_v$  may be scaled out, so that only one

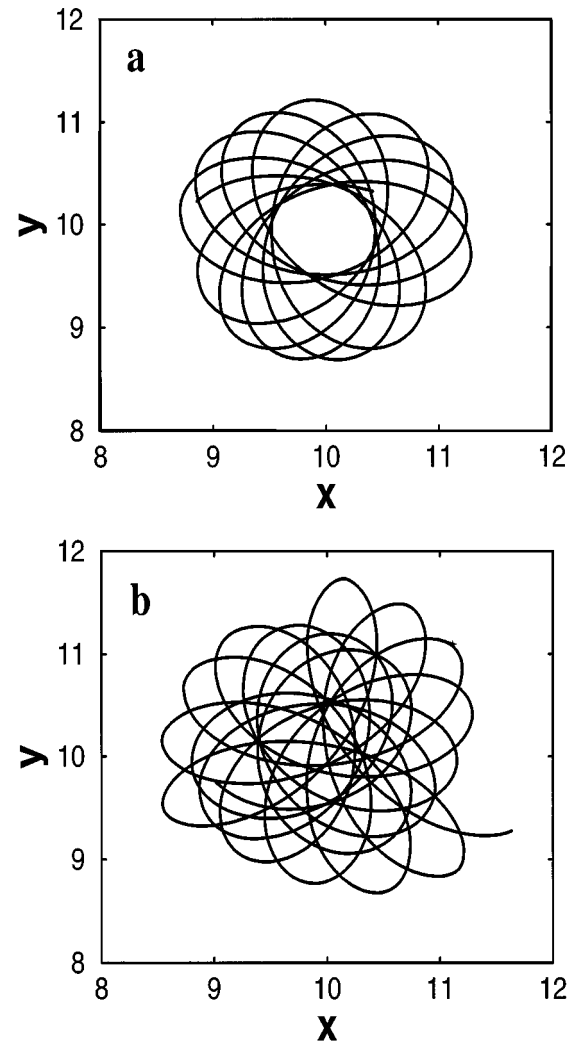


FIG. 2. Trajectory of spiral tip in (a) meandering and (b) hypermeandering regimes. For both cases  $g^+=0.7$ .  $\delta$  is (a) 0.48 and (b) 0.4, respectively. Other parameters are the same as in Fig. 1.

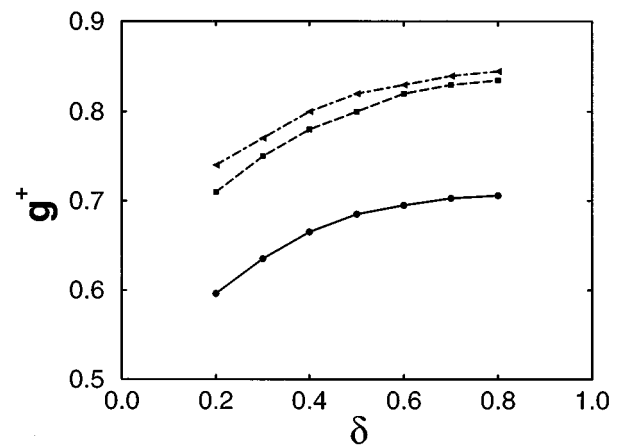


FIG. 3. Lines of core-meander bifurcation in the  $\delta$ - $g^+$  plane. Solid line corresponds to free boundary simulations with the same  $c_v$ , domain size, and number of grid points as in Fig. 1. Dashed and dot-dashed lines correspond to EZ simulations of the original model (1) and (2) with  $\epsilon=0.002$  and  $\epsilon=0.008$ , respectively.

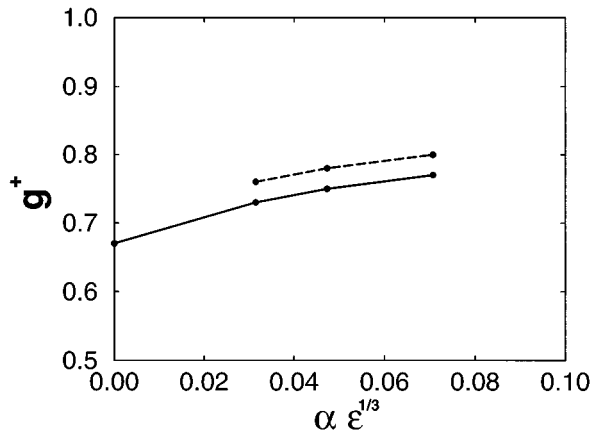


FIG. 4.  $g^+$  at the bifurcation point at various values of  $\alpha\epsilon^{1/3}$  and for  $\delta=0.4$ . Other parameters are the same as in Fig. 1. Solid and dashed lines result from the free boundary simulations and EZ simulations, respectively.

model-dependent parameter  $g^+$  is left. Therefore, we can change  $v$ ,  $x$ ,  $t$ , and  $c_v$  in such a way that in rescaled variables Barkley's model will have  $c_v = -1/\sqrt{2}$ , but the constant  $\alpha$  will be rescaled. Straightforward calculations result in  $\alpha = (a/2)^{2/3}$ .

In Fig. 4 we compare the results of the simulations of the modified (including the  $-\alpha\epsilon^{1/3}v$  term) model (4) and (5) with the results of the EZ simulations of the original model (1) and (2) for various values of  $\alpha$ . One can see a significant improvement with respect to the prior results for  $\alpha=0$ .

## V. CONCLUSION

We have presented the numerical evidence that the finite diffusion free boundary problem is sufficient and consistent for the description of spiral waves in generic reaction-diffusion excitable media. We have found by direct numerical simulations a transition to steady meandering of the spiral core via a supercritical Hopf bifurcation. We have observed a transition to hypermeandering and final breakup of the spiral wave when the diffusion of the slow variable decreases. Thus we resolve the existing controversy in the theory of spiral waves in the small- $\delta$  limit, predicting always a stationary instability of the spiral's core. We have also shown that the higher-order correction to the free boundary problem due to finite  $\epsilon$  is necessary to achieve quantitative agreement with the results for the reaction-diffusion system (1) and (2). Our results, implemented for a two-component reaction-diffusion system, can be straightforwardly generalized for higher numbers of slow fields. This could be useful to study such phenomena as transversal front instability, transition from lamellar to labyrinthine patterns [21], and spiral competition [22].

## ACKNOWLEDGMENTS

The work of I. A. and D. K. was partly supported by Raschi Foundation. The support of ISF is kindly acknowledged.

## APPENDIX A

We solve the diffusion equation (4) using a pseudospectral approach, which consists of the following procedure. The field  $v$  on the grid is transformed into inverse Fourier space, so that the partial differential equation (4) for  $v(x,y)$  is replaced by a set of ordinary differential equations for its harmonics  $\bar{v}_{k_x,k_y}$ :

$$\partial_t \bar{v}_{k_x,k_y} = \bar{g}_{k_x,k_y} - \delta \hat{\mathbf{k}}^2 \bar{v}_{k_x,k_y}, \quad (\text{A1})$$

where  $\hat{\mathbf{k}} = (k_x, k_y)$  is the corresponding wave vector and  $\bar{g}_{k_x,k_y}$  are the harmonics of  $g^\pm(x,y)$ . One immediately writes down the general solution of Eq. (A1) on the interval  $(t; t + \Delta t)$ :

$$\begin{aligned} \bar{v}_{k_x,k_y}(t + \Delta t) = & e^{-\delta(k_x^2 + k_y^2)\Delta t} \left[ \bar{v}_{k_x,k_y}(t) \right. \\ & \left. + \int_t^{t+\Delta t} dt' \bar{g}_{k_x,k_y}(t') e^{\delta(k_x^2 + k_y^2)(t'-t)} \right]. \end{aligned} \quad (\text{A2})$$

By virtue of the small value of  $\Delta t$  this turns into the implicit difference scheme (in the trapezoid approximation)

$$\begin{aligned} \bar{v}_{k_x,k_y}(t + \Delta t) = & e^{-\delta(k_x^2 + k_y^2)\Delta t} \left[ \bar{v}_{k_x,k_y}(t) + \frac{\Delta t}{2} \bar{g}_{k_x,k_y}(t) \right] \\ & + \frac{\Delta t}{2} \bar{g}_{k_x,k_y}(t + \Delta t). \end{aligned} \quad (\text{A3})$$

In order to find  $v(t + \Delta t)$ , one has to calculate  $\bar{v}(t)$ , the Fourier representation of  $v(t)$ , then calculate  $\bar{v}(t + \Delta t)$  according to (A3), and then return to real space. This procedure, however, remains unclosed without consistent updating of the interface to determine the function  $g^\pm(x,y)$ . This problem requires careful consideration.

We proceed in the following way. Initially the 2D function  $g^\pm(x,y)$  is formed by setting it to be  $g^+$  at the ‘‘internal’’ (excited) and  $g^-$  at the ‘‘external’’ (quiescent) grid points and its Fourier representations  $\bar{g}_{k_x,k_y}$  are calculated given the fixed position of the interface.

The outer normal  $\mathbf{n}^i = (n_x^i, n_y^i)$  and curvature  $k^i$  of the interface are calculated at the  $i$ th interfacial point as functions of arclength  $s^i$  through the derivatives of the coordinates  $x$  and  $y$  at the interface with respect to  $s$ , using cubic spline interpolation:

$$\begin{aligned} n_x^i &= \frac{y^{i+1} - y^i}{s^{i+1} - s^i} - \left( \frac{y_{ss}^i}{3} + \frac{y^{i+1}}{6} \right) (s^{i+1} - s^i), \\ n_y^i &= -\frac{x^{i+1} - x^i}{s^{i+1} - s^i} + \left( \frac{x_{ss}^i}{3} + \frac{x^{i+1}}{6} \right) (s^{i+1} - s^i), \\ k^i &= n_y^i y_{ss}^i - n_x^i x_{ss}^i. \end{aligned} \quad (\text{A4})$$

As a next step, the field  $v$  at the gridpoints is updated according to the pseudospectral procedure described above. Fourier transformations are performed by a real cosine fast Fourier transform routine (because of the no-flux boundary

conditions). Then values of  $v$  at the interfacial points are found using bilinear (or bicubic) interpolation between nearest grid points. At this stage one has all the information needed to calculate the new position of the interface according to Eq. (5). This is done by calculating the shift of each interfacial point in the direction of the outer normal by the

distance  $c_n \Delta t$ . We do not need to perform the time-consuming procedure of “filling up” the lattice with  $g^\pm$ 's at each time step. Instead, we change the values of the function  $g^\pm(x,y)$  from  $g^+ \text{ to } g^-$ , and vice versa, at the grid points within the narrow band between the old and the new positions of the interface.

- 
- [1] G.S. Skinner and H.L. Swinney, *Physica D* **48**, 1 (1991); T. Plesser, S.C. Müller, and B. Hess, *J. Phys. Chem.* **94**, 7501 (1990); J. Ross, S.C. Müller, and C. Vidal, *Science* **240**, 460 (1988).
- [2] S. Jakubith, H.H. Rotermund, W. Engel, A. von Oertzen, and G. Ertl, *Phys. Rev. Lett.* **65**, 3013 (1990); B.C. Sales, J.E. Turner, and M.B. Maple, *Surf. Sci.* **114**, 381 (1982).
- [3] M.A. Allesie, F.I.M. Bonke, and F.J.G. Schopman, *Circ. Res.* **33**, 54 (1973); **39**, 168 (1976); **41**, 9 (1977).
- [4] W.F. Loomis, *The Development of Dictyostelium Discoideum* (Academic, New York, 1982).
- [5] D.A. Kessler, H. Levine, and W.N. Reynolds, *Phys. Rev. A* **46**, 5264 (1992); *Physica D* **70**, 115 (1994).
- [6] A. Karma, *Phys. Rev. Lett.* **68**, 397 (1992); **71**, 1103 (1993).
- [7] J.J. Tyson and J.P. Keener, *Physica D* **32**, 327 (1988).
- [8] D.A. Kessler and H. Levine, *Physica D* **39**, 1 (1989).
- [9] J.S. Nagumo *et al.*, *Proc. IRE* **50**, 509 (1979).
- [10] A. Winfree, *CHAOS* **1**, 303 (1991).
- [11] D. Barkley, *Physica D* **49**, 61 (1991).
- [12] D. Barkley, *Phys. Rev. Lett.* **68**, 2090 (1992); **72**, 164 (1994).
- [13] P.C. Fife, *Non-Equilibrium Dynamics in Chemical Systems*, edited by C. Vidal and A. Pacault (Springer, New York, 1984).
- [14] A.J. Bernoff, *Physica D* **53**, 125 (1991).
- [15] D.A. Kessler and R. Kupferman, *Physica D* (to be published).
- [16] D.A. Kessler and R. Kupferman (unpublished).
- [17] I. Aranson, L. Kramer, and A. Weber, *Phys. Rev. Lett.* **72**, 2561 (1994).
- [18] D. Kessler, J. Koplik, and H. Levine, *Adv. Phys.* **37**, 255 (1988).
- [19] D.M. Petrich and R.E. Goldstein, *Phys. Rev. Lett.* **72**, 1120 (1994).
- [20] I. Aranson, D. Kessler, and I. Mitkov, *Phys. Rev. E* **50**, R2395 (1994); *Physica D* **85**, 142 (1995).
- [21] M. Seul and R. Wolfe, *Phys. Rev. Lett.* **68**, 2460 (1992).
- [22] I. Aranson, H. Levine, and L. Tsimring, *Phys. Rev. Lett.* **76**, 1170 (1996).